5-2023

FBH1-deficient cells exhibit a dampened stress response to WEE1 inhibition

Lucy Jennings

FBH1-deficient cells exhibit a dampened stress response to WEE1 inhibition

Lucy Jennings, Dr. Heather Walters, Dr. Jennifer Mason

Abstract

Cancer is defined by uncontrolled growth from irregular activity by cell cycle proteins; recently, some cell cycle regulators have become attractive targets for cancer therapies. One of these targets is WEE1, a tyrosine kinase that phosphorylates tyrosine 15 (Y15) on CDK1 to stop the progression from G2 into mitosis. FBH1 is a DNA helicase critical for the induction of apoptosis in response to replication stress. Importantly, FBH1 is lost in many melanomas. FBH1 cooperates with MUS81 to create double-strand breaks and induce cell death. We hypothesized that the replication stress response in FBH1-deficient cells depends on the WEE1-dependent G2/M checkpoint to repair the damage before entering mitosis; therefore, it could be used as a potential chemotherapeutic option. We examined genome stability in response to the inhibition of WEE1 (AZD1775) by measuring nuclear abnormalities and gamma-H2AX staining. We also measured double-strand break formation after WEE1i treatment using the TUNEL assay. Lastly, we measured the sensitivity of U2OS cells to WEE1i treatment using the Cell titer blue assay. We found that FBH1-deficient U2OS cells possessed increased double-strand breaks, increased mitotic catastrophe, and increased pan-nuclear gamma-H2AX staining in abnormal nuclei. However, this dampened response did not lead to resistance to WEE1 inhibition, as FBH1-deficient cells were more sensitive to WEE1 inhibition. These data suggest that FBH1-deficient cells are more sensitive to WEE1i treatment and ultimately depend on the G2/M checkpoint to repair damages. Future studies will address the response of FBH1 to WEE1i when combined with other treatments like hydroxyurea.

Introduction

The cell cycle is a highly organized and stringent process that ensures DNA is replicated and divided correctly. However, when cells enter mitosis with high levels of replication damage, the cell cycle fails, and these cells undergo mitotic catastrophe and cell death. Cancer cells are characterized by defects in the cell cycle program, exhibiting high levels of replication stress and damage accumulated through DNA repair defects and oncogene expression (1). Usually, in response to replication damage, cells arrest at the G2/M checkpoint to allow repair before progressing into mitosis. Due to high levels of replication stress, cancer cells rely on cell cycle checkpoints to continue proliferation. An emerging chemotherapeutic treatment is to target cell cycle checkpoints in cancer cells with high levels of replication stress to force them prematurely into mitosis and lead to cell death (2)

One of the targets of cell cycle checkpoints is WEE1. WEE1 is a tyrosine kinase that phosphorylates tyrosine 15 (Y15) on CDK1 to inactive it. If damage in the cell is detected, WEE1 stops the progression from G2 into mitosis by phosphorylating the Y15 residue on CDK1 (3). If no DNA damage is detected, CDC25 counteracts WEE1 and removes the phosphate from Y15 to reactivate CDK1. WEE1 also plays a role in S-phase inactivating CDK2, but this project's focus was its role with the G2/M checkpoint. Given the role that WEE1 plays in the progression

into mitosis, inhibition of WEE1 is a promising new chemotherapeutic target for cancer cells that experience high replication stress and damage. WEE1 inhibitors have been developed and shown to kill tumor cells alone or combined with standard chemotherapy when patients are unresponsive to all standard chemotherapy (4). However, compared to traditional treatments, an increase in adverse side effects from Wee1 inhibitor AZD1775 (WEE1i) in patients in clinical trials has reduced its clinical use. Further research is needed to determine the quantity of WEE1i to be used when coupled with other treatments and when it is used for maintenance therapy to keep cancer from returning (4). The conflicting success of WEE1 inhibition in clinical trials shows the need for a better understanding of the genetic alterations that regulate the response to WEE1 inhibition.

DNA is highly susceptible to various factors that can cause damage during replication. When replication forks are under stress or encounter damaged DNA, they stall; these structures then regress to form a new 4-way junction called a chicken fork (5). The new structure protects the stalled fork from being cleaved and protects the DNA's integrity by avoiding potentially mutagenic DNA damage tolerance pathways (DDT). The regressed forks are stabilized by an array of proteins used in double-strand break repair and homologous recombination (HR). One of these proteins is FBH1, a UvrD helicase that works alongside a nuclease, MUS81, to create a double-strand break when cells have been experiencing prolonged stress (6). FBH1-deficient cells have decreased double-strand break formation and increased survival in response to hydroxyurea and ultraviolet (UV) light. FBH1 has anti-cancer functions at replication forks by protecting melanocytes from UV-mediated transformation. Hemizygous and homozygous loss of FBH1 was found in up to 55% of melanoma cell lines (7).

Since FBH1 is critical in promoting cleavage of replication forks using MUS81, we sought to determine how a deficiency in FBH1 affects the cellular response to WEE1 inhibition. We found U2OS-FBH1 KO cells result in a reduction in break signaling, indicating FBH1 is required for the efficient induction of the replication stress response to WEE1i. We also found that FBH1 KO cells had increased sensitivity and reduced growth in response to WEE1i. However, WEE1i resulted in significant nuclear aberrations that stained positively for gamma H2AX (yH2AX), indicating WEE1i inhibition resulted in increased mitotic catastrophe. We propose that the underlying defect in replication stress response results in dependency on the WEE1-dependent checkpoint.

Materials and Methods

Cell lines and drug treatments. U2OS and U2OS FBH1 knockout cells were grown in DMEM (Gibco Cat #11965-092) media +10% FBS (EqualFetal, Atlas Biologicals) and were cultured at 37ºC, 5% CO2. AZD1775 (MedChemExpress) was resuspended in DMSO. Cells were treated with AZD1775 as indicated.

Immunofluorescence. U2OS and FBH1 KO (50,000) cells were plated on coverslips in a 12-well tissue culture plate and grown overnight. Cells were treated with various concentrations

of AZD1775 or DMSO (vehicle control) at the indicated time points. Cells were permeabilized, and cytosol was extracted by incubating coverslips in 1 mL of pre-extraction buffer (20 mM HEPES, ph7.4, 0.5% TritonX-100, 50 mM NaCl, 3 mM MgCl2, 300 mM sucrose) for 10 min at RT. Cells were washed with 1 mL of 1X PBS and then fixed by incubating coverslips in 3% paraformaldehyde with 3.4% sucrose in 1X PBS for 10 min at RT. Cells were washed with 1 mL 1X PBS 3 times and then were incubated in 3% bovine serum albumin in PBS (BSA, Fisher cat# BP1605-100) (w/v) for 20 min at RT. Primary antibodies were diluted in 1% BSA, added to coverslips in a humidified glass chamber, and incubated overnight at 4°C. Cells were washed 3 times with 1 mL 1X PBS and then incubated with appropriate AlexaFluor secondary antibodies diluted 1:1000 diluted 1:1000 in 1% BSA in a humidified glass chamber, in the dark, at RT for 1 hour. Cells were washed 3 times in 1X PBS, and dehydrated by incubating for 2 min in increasing concentrations of EtOH (70%, 95%, and 100%) before mounting with Vectashield with DAPI (Fisher, cat #NC9524612). Images were scored using Fiji software (version 1.53v, NIH), and data were analyzed and graphed using GraphPad Prism software (version 9.5.0, Dotmatics).

Antibodies. mouse anti- phosphorylated-γH2AX (Abcam, Cat# ab26350) and anti-phosphorylated histone H3 (Abcam, cat# ab5176, 1:1000)
Secondary antibodies: Alexafluor 488 (Fisher, cat# A11001) and AlexaFluor 594 (Fisher, cat# A11037).

Wee1 Inhibitor Dose Curve. U2OS or FBH1 KO (100,000) cells were plated on coverslips in 12-well tissue culture and grown overnight. Cells were treated with 0, 100, 200, 400, 800, or 1000 nM of WEE1i or DMSO for 24hrs. Cells were permeabilized and fixed, as described above. No primary or secondary staining with antibodies was needed. Cells were dehydrated and mounted with Vectashield with DAPI as described above in Immunofluorescence. Images were scored using Fiji software (version 1.53v, NIH), and data were analyzed and graphed using GraphPad Prism software (version 9.5.0, Dotmatics).

Western Blotting. Western blotting of whole-cell lysates was used to assess protein expression. Cells were trypsinized and pelleted by centrifugation at 500 × g for 5 min. Cells were resuspended in 1X PBS (Gibco, Cat #20012-027) and enumerated using a hemocytometer and light microscopy. Cells were pelleted again by centrifugation at 500 × g and lysed at 106 cells/100 µL 1X SDS lysis buffer (0.0625M Tris-HCL pH 6.8, 2% SDS, 10% glycerol, 01M DTT, and 0.1 mg/mL bromophenol blue). Samples were heated for 5 min at 100°C and loaded onto a 10% SDS-PAGE gel. The gels were electrophoresed in 1X running buffer (25 mM Tris, 1.92 mM glycine, and 0.1% SDS) at 125V for approximately 60 min. Proteins were then transferred to polyvinylidene difluoride (PVDF) membranes (Biorad, cat#1620177) at 100V for 1 h in 1X transfer buffer (25 mM Tris, 192 mM glycine, 20% [vol/vol] methanol). Membranes were blocked with 5% (wt/vol) powdered milk (Nestle Carnation) dissolved in TBST (10 mM Tris, 150 mM NaCl, 1% [vol/vol] Tween 20 (Fisher, Cat# BP337-100)) for 1 h at RT. Membranes were incubated overnight at 4°C in primary antibodies diluted in TBST. anti-FBH1 (1:100, Pacific Immunology), pCDK (Abcam ab275958), or anti-Tubulin (Novus Biologicals, cat# NB100-690). Membranes were washed in TBST for 30 min with 3 buffer changes and incubated in commercially available horseradish peroxidase-conjugated goat anti-rabbit or goat anti-mouse

antibody (Licor WesternSure, cat#926-80011 and cat#926-80010; diluted 1:2,000 in 5% powdered milk in TBST) for 1 hr at room temperature and extensively washed as described above. According to the manufacturer's instructions, all blots were developed using a commercially available enhanced chemiluminescence Western blotting detection system (Licor Westernsure, cat# 926-95000). To measure expression levels of total versions of CDK (Abcam cat# ab32094), original membranes were stripped for 30 min with 2 buffer changes with a mild stripping buffer (15 mg/mL glycine, 1 mg/mL SDS, 10% Tween 20, pH adjusted to 2.2 using concentrated HCL). Before probing with antibodies overnight at 4°C, membranes were blocked in 5% milk in TBST.

TUNEL Assay. To detect apoptosis in response to Wee1 Inhibition in U2OS and FBH1 KO cells, 50,000 cells per sample were plated on round coverslips in a 12-well plate and grown overnight. Cells were then treated with 400nM AZD1775 or DMSO (vehicle control) for 24hr. Cells were permeabilized and fixed using the same technique in Immunostaining. We used the Click-It Plus TUNEL Assay to stain the coverslips as directed (Invitrogen, C10617, C10618, C10619). Coverslips were placed in a humidified glass chamber, and 100ul of TdT Reaction Buffer was added to each coverslip and incubated at 37℃ for 10 minutes. Cells were washed with 1X PBS to remove the TdT Reaction Buffer. Next, a TdT reaction mixture was prepared. For each coverslip, there was 47ul of TdT Reaction Buffer, 1ul of EdUTP, and 2ul of TdT enzyme. 50ul of the TdT reaction mixture was added to each coverslip and incubated in a humidified glass chamber for 60 minutes at 37℃. Cells were washed twice with 3% BSA in PBS for 5 minutes each. Next, cells undergo a Click-iT Plus reaction. A 10X Click-iT Plus TUNEL Reaction Buffer Additive was prepared by diluting the 100X solution 1:10 in DI water. Prepare the Click-iT Plus TUNEL reaction cocktail using the 10X Click-iT Plus TUNEL Reaction Buffer Additive. For each coverslip, you need 45ul for Click-iT Plus TUNEL Supermix and 5ul of 10X Click-iT Plus TUNEL Reaction Buffer Additive; immediately after making the cocktail add 50ul to each coverslip and incubate in a humidified glass chamber for 30 minutes, at 37℃, protected from light. Cells were washed with DI water and washed with 3% BSA for 5 minutes. Cells were washed with 1X PBS, and dehydrated by incubating for 2 minutes in increasing concentrations of EtOH (70%, 95%, and 100%) before mounting with Vectashield with DAPI. Images were scored using Fiji software.

Cell titer blue assay. U2OS or FBH1-KO cells were plated in triplicate at various concentrations: 1000, 500, 250, and 125 cells in a 96-well plate (3904, Corning) and grown overnight. Cells were treated with either DMSO or 400nM AZD1775 for 48 hr. To perform the cell titer blue assay, 20 µl of CellTiter-Blue Reagent (G8088, Promega) was added to each well and incubated for 2 hours at 37°C. 50 µL of 3% SDS was added to each well to stop the reaction. The Fluorescence of each sample was read at an excitation of 570 nm and emission of 600 nm while shaking for 10 seconds. The mean of each set of triplicates was calculated. Sample values were normalized by dividing each value by its corresponding untreated sample value and plotted as percent cell survival.

Results

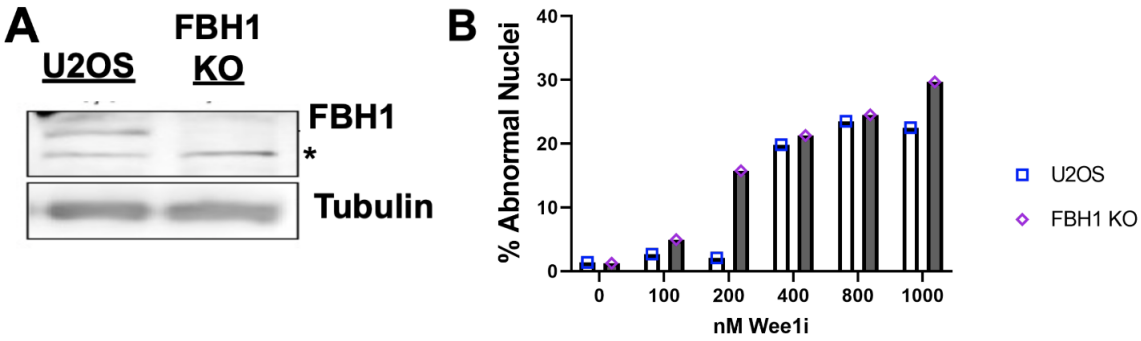

Figure 1. A) Western Blot Analysis of levels of FBH1 in U2OS cells (control) and CRISPR-Cas9 created knockout. Tubulin serves as a loading control. B) Dosage Curve of WEE1i in U2OS and FBH1 KO cells to determine the most effective concentration for future experiments.

Generation of FBH1 KO cell line and determination of effective WEE1i concentration

To determine how FBH1-deficient cells respond to the inhibition of WEE1, we knocked out FBH1 in U2OS cells and confirmed the KO using Western Blot analysis (Fig 1A). Due to the unknown potential effect of WEE1i on the cells, a dosage curve was conducted to determine the most efficient concentration for disrupting normal cell cycle regulation. There was a significant increase in disruption of the cell cycle in FBH1 KO cells at 200nM of WEE1i compared to U2OS, seemingly the most efficient concentration of WEE1i (Fig 1B). However, we chose to move forward in future experiments using 400nM of WEE1i because we were not detecting signals of replication response with 200nM. Instead, we were able to induce the replication response with 400nM.

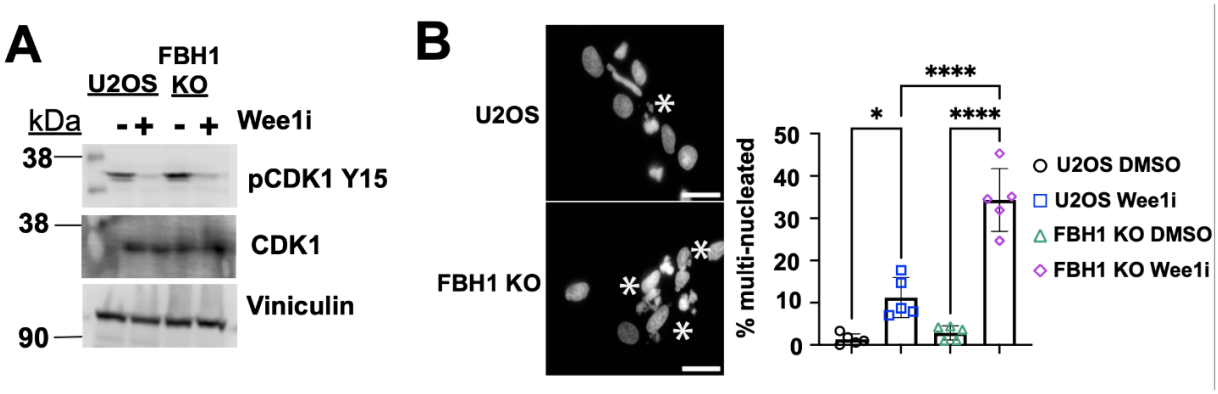

Figure 2. A) Western Blot analysis of the effectiveness of Wee1 inhibition in U2OS and FBH1 KO cell lines. Viniculin serves as a loading control. B) Images and a bar graph showing the nuclear abnormalities occurring to U2OS and FBH1 KO cells after 24hr WEE1i treatment.

Treatment of FBH1 KO cells with WEE1i increases genome instability

U2OS and FBH1 KO cells were treated with WEE1i for 24hrs. After treatment, U2OS and FBH1 KO cells had significantly reduced levels of CDK1 phosphorylation at position Y15. This decreased phosphorylation level showed efficient inhibition of WEE1 (Fig 2A). The level of CDK and Viniculin was also checked as controls. In cancerous cells, when they are forced into mitosis with DNA damage, they undergo mitotic catastrophe and cell death (8). A characteristic of mitotic catastrophe is the multinucleation of the cells. After treatment with WEE1i for 24hrs, we examined nuclear abnormalities. In U2OS cells, WEE1i significantly increased the percentage of multinucleated cells from 1.3% to 11.2%. Strikingly, FBH1 KO cells exhibited a 3-fold increase in multinucleated cells after Wee1i treatment (34.3% cells) compared to U2OS, suggesting that FBH1 prevents mitotic catastrophe after WEE1 inhibition (Fig 2B).

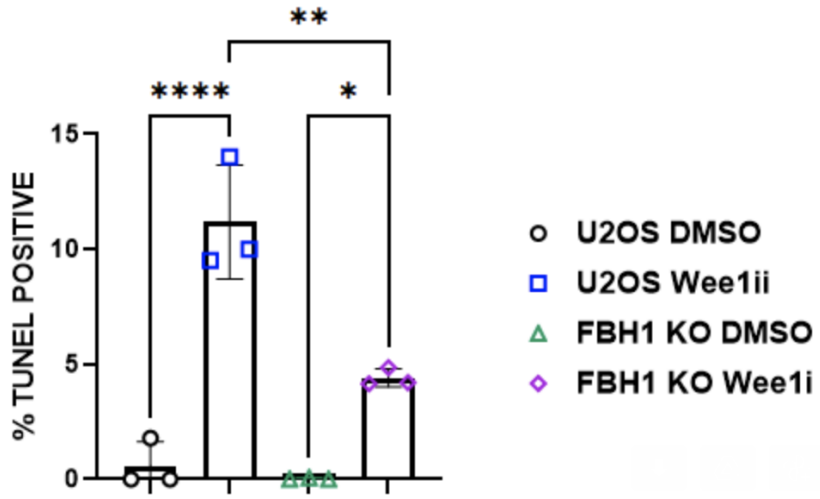

Figure 3. Bar graph showing the % of TUNEL positive U2OS and FBH1 KO cells after 24hr treatment with WEE1i. Bars represent an average of three independent experiments. Error bars are standard deviations. ****p<0.0001, *p<0.0175, **p<0.0013, ANOVA with Tukey HSD.

FBH1 is required for double-strand break formation after WEE1i inhibition

WEE1 inhibition results in unrestrained cleavage by the endonuclease MUS81/SLX4 (9). In response to hydroxyurea, FBH1 promotes MUS81-dependent cleavage of replication forks. We determined if FBH1 promotes double-strand break formation after treatment with WEE1i using the TUNEL assay (10). In U2OS cells, WEE1i treatment increased the percentage of TUNEL-positive cells (18-fold), indicating double-strand break formation (Figure 3). In FBH1 KO cells treated with WEE1i, we observed a 2.5-fold reduction in TUNEL-positive cells compared to U2OS, indicating FBH1 promotes efficient cleavage of replication forks.

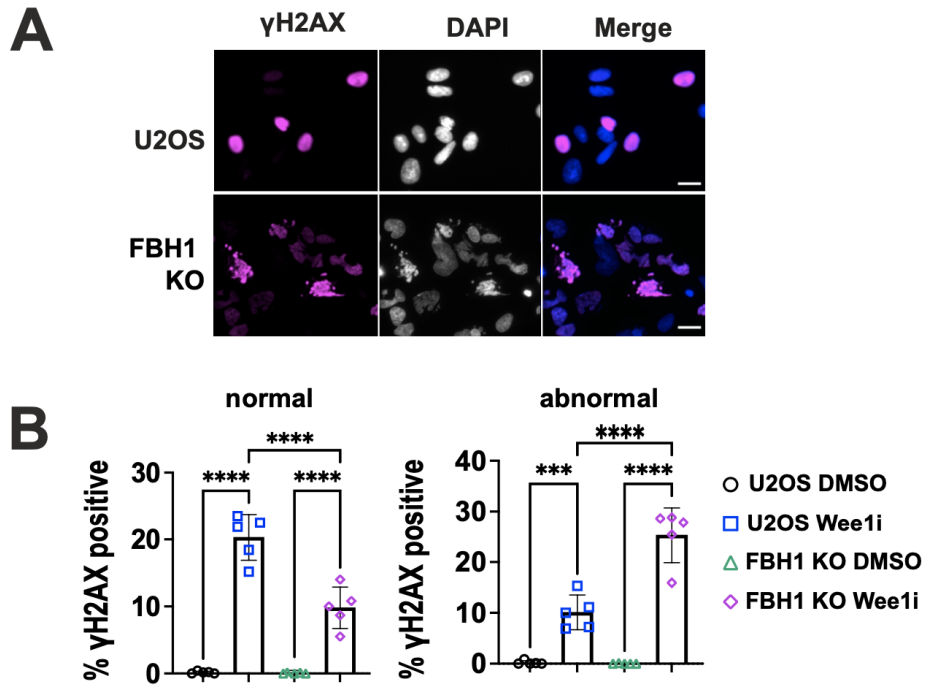

Figure 4. A) Images of U2OS and FBH1 KO cells after 24hr treatment with WEE1i. B) Bar graph of % γH2AX positive U2OS and FBH1 KO cells in normal nuclei (replication stress) and abnormal nuclei (mitotic catastrophe). Bar graphs represent the average of each experiment with individual data points depicted. ***p<0.0005, ****p<0.00005, ANOVA with Tukey HSD.

Wee1i treatment leads to two distinct pan-nuclear γH2AX populations in U2OS cells

The histone H2AX is phosphorylated at Ser139 in response to DNA damage to form immunostaining foci. In cells undergoing replication catastrophe or apoptosis, nuclei exhibit intense γH2AX staining, known as pan-nuclear staining (11). Previous studies have shown that FBH1-deficient cells significantly reduce pan-nuclear γH2AX in response to replication stress caused by hydroxyurea treatment. We measured the induction of pan-nuclear γH2AX in U2OS

and FBH1 KO cells after treatment with WEE1i. We observed significant differences in the nuclei staining positive for pan-nuclear γH2AX in U2OS and FBH1 KO cells. Of the 30% γH2AX positive cells in U2OS cells, 20% (60% of the γH2AX positive population) occurred in nuclei without aberrations (i.e., normal). Of the 33.7% γH2AX positive nuclei in FBH1 KO cells, 25.3% (70.4% of the γH2AX positive cells) occurred in multi-nucleated cells.
These results indicate that pan-nuclear H2AX is arising due to distinct mechanisms. In U2OS, γH2AX is forming as a result of replication stress. In FBH1 KO, γH2AX occurs due to mitotic catastrophe.

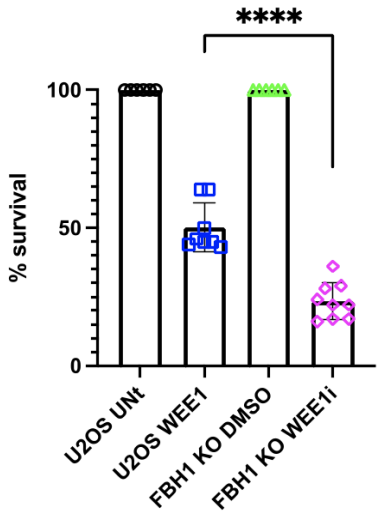

Figure 5. Bar graph showing % survival of U2OS and FBH1 KO cells after 48hr treatment with WEE1i and a 4-5 day outgrowth. Bar graphs represent the average of each experiment with individual data points depicted. ****p<0.00005, ANOVA with Tukey HSD.

FBH1 KO cells exhibit reduced growth in response to WEE1i
Cell survival was measured by allowing cells to grow after treatment with WEE1i. In U2OS, WEE1i resulted in a 49.9% reduction in survival compared to the untreated control. FBH1 KO cells were more sensitive to WEE1i and exhibited a 76.6% reduction in cell survival compared to the untreated control. A 2-fold difference in survival between U2OS and FBH1 KO cells. These results suggested that FBH1 KO U2OS cells are more sensitive to Wee1i.

Discussion

FBH1 is critical for the induction of apoptosis in response to replication stress. FBH1 promotes fork regression and double-strand break formation using MUS81 when severe enough replication stress occurs (12). Given the resistant nature of FBH1-deficient cells to UV and hydroxyurea, we aimed to determine how FBH1-deficiency could modulate the cellular response to WEE1 inhibition.

Our results show FBH1 is required to promote the cellular response to replication stress induced by WEE1 inhibition. In cells with damaged or under-replicated DNA, WEE1 activates the G2-M checkpoint to allow cells sufficient time to repair (3). When WEE1 becomes inactive, cells with damaged DNA prematurely enter mitosis, resulting in mitotic catastrophe. In U2OS

cells, FBH1-deficiency resulted in a significant increase in multi-nucleation consistent with mitotic catastrophe. U2OS cells exhibited much less aberrant nucleation suggesting that FBH1 is helping to prevent mitotic catastrophe in the presence of WEE1 inhibition. These results imply that WEE1 inhibition results in genome instability in FBH1-deficient cells.

FBH1 is necessary for double-strand break formation. Looking at the TUNEL assay, U2OS cells had much higher double-strand break formation than FBH1-deficient cells in response to WEE1 inhibitors. This reduction in double-strand break formation in FBH1-deficient cells suggests that FBH1 plays a similar role in promoting breaks in response to replication stress induced by WEE1 inhibition compared to its response to UV and hydroxyurea.

We see more evidence that FBH1 promotes the cellular response to replication stress caused by WEE1 inhibition through γH2AX staining. FBH1-deficient cells exhibited more γH2AX positive nuclei in abnormal multi-nucleated cells than U2OS in response to WEE1 inhibition. U2OS cells showed more γH2AX positive nuclei in nuclei with no aberrations in response to WEE1 inhibition. These results suggest that in U2OS cells, γH2AX staining was arising due to replication stress. In FBH1-deficient cells, γH2AX staining arises due to mitotic catastrophe. The sensitivity data shows that FBH1-deficient cells are more sensitive to WEE1 inhibition than U2OS cells and die faster.

We propose that the increased sensitivity of FBH1-deficient cells in response to WEE1 inhibition is due to the simultaneous increase in replication stress and loss of the G2/M checkpoint. FBH1 has been implicated in promoting fork reversal in response to replication stress. Previous studies have shown fork reversal suppresses DNA damage tolerance pathways that continue replication in the presence of a drug (13). Fork reversal mediated by HLTF limits progression by FANCM in unperturbed cells and by PRIMPOL and REV1 in cells with high levels of replication stress. PRIMPOL-mediated replication results in ssDNA gaps in replication, and cells depend on post-replication pathways in G2 to fill these gaps (14). Importantly, lesions to the DNA, like gaps and other damage, have been shown to sensitize cells to WEE1i. One possibility is that increased DDT pathways usage in the absence of FBH1 results in lesions such as gaps that escape detection by the replication checkpoint. Due to the loss of fork reversal, we speculate that FBH1 deficient cells rely on the G2/M checkpoint to repair replication-associated DNA lesions. With WEE1 inhibiting CDK1 from arresting cells at this checkpoint, we see more of an effect of WEE1 inhibition on FBH1-deficient cells in the form of more mitotic catastrophe, more γH2AX staining in abnormal nuclei, and more overall cell death.

WEE1 is a complex protein that plays many roles within the cell cycle. As discussed in this paper, one of the main functions is phosphorylating CDK and arresting cells at the G2/M transition for potential repair. However, WEE1 also plays a role at the beginning of the S phase, phosphorylating CDK2 for replication origin firing. Inhibition of this function of WEE1 can result in a depletion of nucleotide pools, accumulation of single-stranded DNA, and subsequent replication catastrophe (3). This additional function of WEE1 is another piece to the story of how FBH1-deficient cells respond to WEE1 inhibition and is currently being investigated by Dr. Heather Walters, a postdoc in my lab. We saw that FBH1-deficient cells exhibit a dampened stress response to WEE1 inhibition, unable to go through the correct MUS81 fork breakage and double-strand break signaling steps. A future direction of this project is to see how these FBH1-deficient cells would respond to a synergized treatment of WEE1 inhibition and hydroxyurea to provide more answers on how FBH1 promotes the cellular response to replication stress induced by WEE1 inhibition.

References

1. Otto T, Sicinski P. Cell cycle proteins as promising targets in cancer therapy. Nat Rev Cancer. 2017 Jan 27;17(2):93-115. doi: 10.1038/nrc.2016.138. PMID: 28127048; PMCID: PMC5345933.
2. Nickoloff JA. Targeting Replication Stress Response Pathways to Enhance Genotoxic Chemo- and Radiotherapy. Molecules. 2022 Jul 25;27(15):4736. doi: 10.3390/molecules27154736. PMID: 35897913; PMCID: PMC9330692.
3. Elbæk CR, Petrosius V, Sørensen CS. WEE1 kinase limits CDK activities to safeguard DNA replication and mitotic entry. Mutat Res. 2020 Jan-Apr;819-820:111694. doi: 10.1016/j.mrfmmm.2020.111694. Epub 2020 Feb 25. PMID: 32120135.
4. Meng X, Gao JZ, Gomendoza SMT, Li JW, Yang S. Recent Advances of WEE1 Inhibitors and Statins in Cancers With p53 Mutations. Front Med (Lausanne). 2021 Oct 4;8:737951. doi: 10.3389/fmed.2021.737951. PMID: 34671620; PMCID: PMC8520942.
5. Berti M, Cortez D, Lopes M. The plasticity of DNA replication forks in response to clinically relevant genotoxic stress. Nat Rev Mol Cell Biol. 2020 Oct;21(10):633-651. doi: 10.1038/s41580-020-0257-5. Epub 2020 Jul 1. PMID: 32612242.
6. Fugger K, Mistrik M, Neelsen KJ, Yao Q, Zellweger R, Kousholt AN, Haahr P, Chu WK, Bartek J, Lopes M, Hickson ID, Sørensen CS. FBH1 Catalyzes Regression of Stalled Replication Forks. Cell Rep. 2015 Mar 17;10(10):1749-1757. doi: 10.1016/j.celrep.2015.02.028. Epub 2015 Mar 12. PMID: 25772361.
7. Jeong YT, Cermak L, Guijarro MV, Hernando E, Pagano M. FBH1 protects melanocytes from transformation and is deregulated in melanomas. Cell Cycle. 2013 Apr 1;12(7):1128-32. doi: 10.4161/cc.24165. Epub 2013 Mar 6. PMID: 23466708; PMCID: PMC3646868.
8. Castedo, M., Perfettini, JL., Roumier, T. *et al.* Cell death by mitotic catastrophe: a molecular definition. *Oncogene* 23, 2825–2837 (2004). https://doi.org/10.1038/sj.onc.1207528
9. Kim SM, Forsburg SL. Regulation of Structure-Specific Endonucleases in Replication Stress. Genes (Basel). 2018 Dec 14;9(12):634. doi: 10.3390/genes9120634. PMID: 30558228; PMCID: PMC6316474.
10. Toledo LI, Altmeyer M, Rask MB, Lukas C, Larsen DH, Povlsen LK, Bekker-Jensen S, Mailand N, Bartek J, Lukas J. ATR prohibits replication catastrophe by preventing global exhaustion of RPA. Cell. 2013 Nov 21;155(5):1088-103. doi: 10.1016/j.cell.2013.10.043. Erratum in: Cell. 2014 Jan 16;156(1-2):374. PMID: 24267891.
11. Moeglin E, Desplancq D, Conic S, Oulad-Abdelghani M, Stoessel A, Chiper M, Vigneron M, Didier P, Tora L, Weiss E. Uniform Widespread Nuclear Phosphorylation of Histone H2AX Is an Indicator of Lethal DNA Replication Stress. Cancers (Basel). 2019 Mar 13;11(3):355. doi: 10.3390/cancers11030355. PMID: 30871194; PMCID: PMC6468890.

12. Fugger K, Chu WK, Haahr P, Kousholt AN, Beck H, Payne MJ, Hanada K, Hickson ID, Sørensen CS. FBH1 co-operates with MUS81 in inducing DNA double-strand breaks and cell death following replication stress. Nat Commun. 2013;4:1423. doi: 10.1038/ncomms2395. PMID: 23361013.
13. Quinet A, Tirman S, Cybulla E, Meroni A, Vindigni A. To skip or not to skip: choosing repriming to tolerate DNA damage. Mol Cell. 2021 Feb 18;81(4):649-658. doi: 10.1016/j.molcel.2021.01.012. Epub 2021 Jan 29. PMID: 33515486; PMCID: PMC7935405.
14. Piberger, A.L., Bowry, A., Kelly, R.D.W. *et al.* PrimPol-dependent single-stranded gap formation mediates homologous recombination at bulky DNA adducts. *Nat Commun* 11, 5863 (2020). https://doi.org/10.1038/s41467-020-19570-7